

Supporting Information

Amorphous Co(OH)₂ Nanocages Achieving Efficient Photo-Induced Charge Transfer for Significant SERS Activity

*Jian Yu,^{‡a} Chao Chen,^{‡c} Jie Lin,^{*ab} Xiangyu Meng,^a Lin Qiu^{*d} and Xiaotian Wang^{*a}*

^aSchool of Chemistry, Beihang University, Beijing 100191, China

^bCixi Institute of Biomedical Engineering, Chinese Academy of Science (CAS) Key Laboratory of Magnetic Materials and Devices & Zhejiang Engineering Research Center for Biomedical Materials, Ningbo Institute of Materials Technology and Engineering, CAS, 1219 ZhongGuan West Road, Ningbo 315201, China

^cSchool of Materials Science and Engineering, Nanyang Technological University, 50 Nanyang Avenue, Singapore 639798, Singapore.

^dSchool of Energy and Environmental Engineering, University of Science and Technology Beijing, 100083 Beijing, China

[‡]These authors contributed equally to this work.

*Corresponding author. Email: wangxt@buaa.edu.cn; qiulin@ustb.edu.cn; linjie@nimte.ac.cn

S1 Synthesis Methods

S1.1 Chemicals

Ethanol (>99.9%), Cobalt chloride (CoCl_2), Polyvinyl Pyrrolidone (PVP) (average molecular weight: 30,000). We purchased crystalline CH-Co from Sigma Aldrich, and Carbon papers (0.05 mm) from Jing Long Te Tan Corporation.

S1.2 Synthesis of Octahedral Cu_2O Templates

First of all, the octahedral Cu_2O synthesized were synthesized through our previous method.¹ NaOH aqueous solution (2.0 M, 10 mL) was added into a mixed aqueous solution of 100 mL H_2O , 4.5 g polyvinylpyrrolidone (PVP, K30), and 0.171 g $\text{CuCl}_2 \cdot 2\text{H}_2\text{O}$. The solution's color switched to blue-green and subsequently dark brown. Then the ascorbic acid solution (0.6 M, 10 mL) was added to the above solution after 30 minutes. The Cu_2O with turbid red color was formed by 3 h stirring. The whole process was completed under smooth stirring and heated in the 55 °C water bath. The distilled water and ethanol were used to wash the precipitates 3 times and finally dried out in a vacuum at 60 °C for 10 h.

S1.3 Synthesis of Amorphous $\text{Co}(\text{OH})_2$ Nanocages

1.7 mg $\text{CoCl}_2 \cdot 6\text{H}_2\text{O}$ and 5.0 mg octahedral Cu_2O were added to the mixed solvent of 5 mL water with 0.3333 g PVP and 5 ml ethanol. After stirring and sonication, $\text{Na}_2\text{S}_2\text{O}_3$ aqueous solution (1.0 M, 4.0 mL) was then added dropwise into the uniform solution. The suspension solution's color turned to expected one within certain amount time and we fabricated the amorphous $\text{Co}(\text{OH})_2$ nanocages after centrifugal washing by ethanol (3 times) and deionized water (2 times). All procedure above was performed at room temperature.

S2 Characterization

The morphologies of the synthesized samples were prepared on Si substrates and studied by a JEOL JSM-7500F cold-field emission scanning electron microscope. Electron paramagnetic resonance (X-band EPR, JEOL JES-FA200) was operated at a frequency of 9.835 GHz at 123K. Each test involved a 40 mg sample to measure the oxygen vacancy content of a certain weight. The EPR intensity of each sample was normalized by the intensity of the Mn standard. In the absence of specific instructions,

the EPR measured samples were first subjected to several normal washing procedures with deionized water. High-resolution transmission electron microscopy (HRTEM) and the transmission electron microscopy (TEM) as well as selective area electron diffraction (SAED) pattern analysis were carried out by the field emission transmission electron microscope using JEOL (TEM-2100F). Raman spectra were obtained using a Job800 Yvon Raman spectrometer model HR800 with excitation wavelengths of 514, 633 and 785 nm He-Ne laser lines (laser power: ~ 1 mW; laser spot: $1.5 \mu\text{m}^2$) at room temperature. X-ray photon spectroscopy (XPS) was employed by the Thermo Scientific ESCALAB 250 Xi XPS system with an analysis chamber of 1.5×10^{-9} mbar and an X-ray spot size of $500 \mu\text{m}$.

SERS Measurement: Raman spectra were characterized by Jobin Yvon Raman spectrometer of the model HR800. Laser 514, 633 and 785 nm produced by a He-Ne laser was used as excitation source. The laser spot was $\sim 1.5 \mu\text{m}^2$ and the laser power was ~ 1 mW to the surface of c- and a- $\text{Co}(\text{OH})_2$. The number of gratings in the Raman spectrometer was $600 \text{ grooves mm}^{-1}$. SERS spectra of target molecules adsorbed on the $\text{Co}(\text{OH})_2$ substrates were acquired on silicon wafer backing. The accuracy of the SERS measurements was evaluated by comparing 20 different SERS spots at the same conditions.

S3 Supplementary Figures and Tables

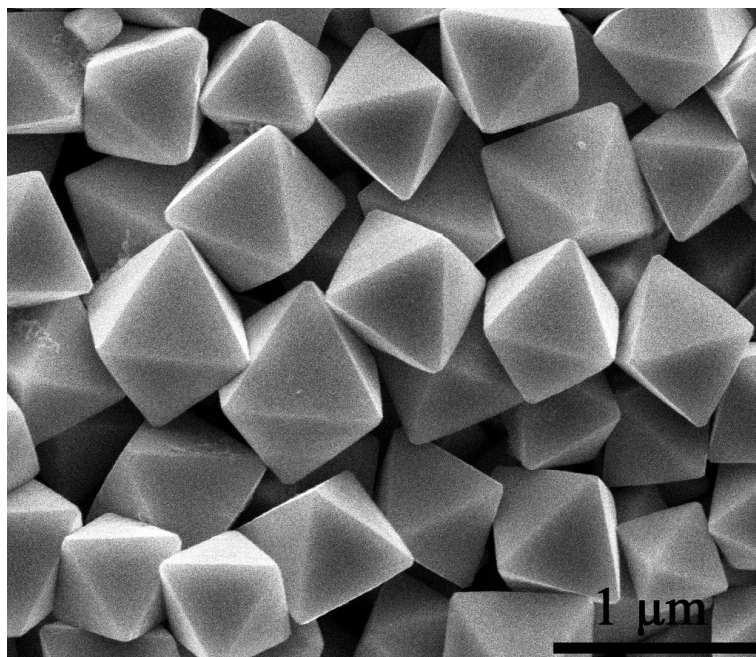


Figure S1. SEM image of crystalline Cu₂O octahedra.

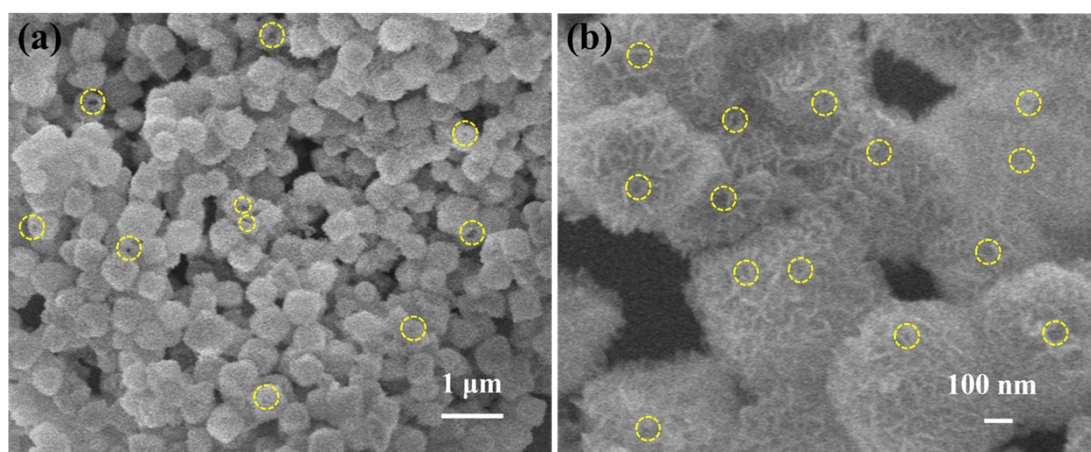


Figure S2. (a,b) SEM image of the a-Co(OH)₂ NCs. The yellow circle represents porous.

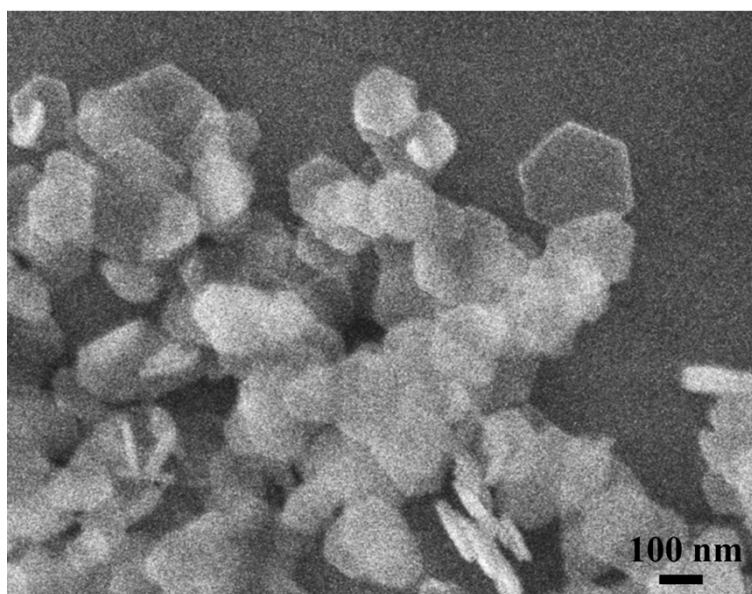


Figure S3. SEM image of the c-Co(OH)₂.

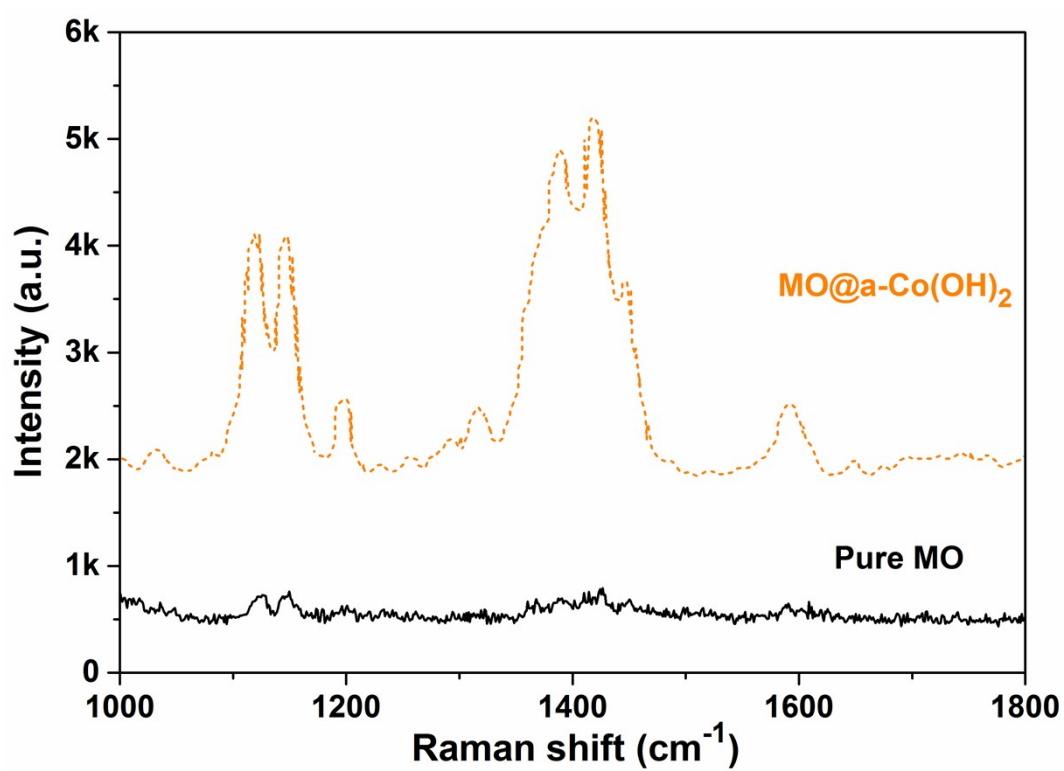


Figure S4. The Raman spectra of MO (1×10^{-6} M) adsorbed on a-Co(OH)₂ NCs substrate and pure MO molecule (0.1 M).

Enhancement factor calculation:

Using a concentration of EB solution below 10^{-4} M to prevent supersaturated adsorption of probe molecules on a-Co(OH)₂ NCs produces false EF values. The EF for a-Co(OH)₂ NCs was calculated by the following equation:

$$EF = (I_{\text{SERS}} / N_{\text{SERS}}) / (I_{\text{bulk}} / N_{\text{bulk}}) \quad (1)$$

In equation (1), N_{SERS} and N_{bulk} represent the number of EB molecules in the SERS sample and the normal Raman sample, respectively. I_{SERS} and I_{bulk} are the same vibration peak of EB molecule on one a-Co(OH)₂ NC and the normal Raman spectrum from pure EB molecule, respectively. In the experiment, The laser spot area is about $1.5 \mu\text{m}^2$. For the normal Raman spectrum, 40 μL pure EB ethanol solution with the concentration of 0.1 mol/L was dried onto the Si wafer and spread into a shape with the area of $\sim 0.5 \times 0.5 \text{ cm}^2$. Avogadro constant (N_A) is $6.02 \times 10^{23} \text{ mol}^{-1}$.

For the N_{bulk} :

$$N_{\text{bulk}} = C \cdot V \cdot N_A \cdot S_{\text{Laser}} / S_{\text{Si}} = 0.1 \text{ mol/L} \cdot 40 \times 10^{-6} \text{ L} \cdot 6.02 \times 10^{23} \text{ mol}^{-1} \cdot 1.5 \mu\text{m}^2 / (25 \times 10^6 \mu\text{m}^2) = 1.445 \times 10^{11}$$

For the N_{SERS} :

$$N_{\text{SERS}} = C' \cdot V' \cdot N_A \cdot S_{\text{eff}} / S_{\text{Si}}$$

Considering that approximately one a-Co(OH)₂ nanocage is under the laser spot, the effective area S_{eff} is equal to the surface area of one a-Co(OH)₂ nanocage ($S_{\text{a-Co(OH)}_2}$). The edge length of the synthesized octahedral Cu₂O is about 600 nm. Therefore, the surface area of one Cu₂O octahedron ($S_{\text{Cu}_2\text{O}}$) is about $1.2 \times 10^6 \text{ nm}^2$. Moreover, the specific surface area of Cu₂O octahedrons and a-Co(OH)₂ nanocages are measured to

be 5.0 m²/g (S_{BET-Cu₂O}) and 20.0 m²/g (S_{BET-a-Co(OH)₂}), respectively (Table S3).

According to:

$$S_{a-Co(OH)_2} / S_{Cu_2O} = S_{BET-a-Co(OH)_2} / S_{BET-Cu_2O}$$

It is deduced that $S_{a-Co(OH)_2} = 4.8 \times 10^6 \text{ nm}^2$. Moreover, 10 μL mixed solution of EB adsorbed on a-Co(OH)₂ NC (MB@ a-Co(OH)₂) is dropped onto $0.5 \times 0.5 \text{ cm}^2$ Si wafer (the concentration of EB is $1 \times 10^{-5} \text{ mol/L}$). Therefore,

$$N_{SERS} = C' \cdot V' \cdot N_A \cdot S_{eff} / S_{Si} = C' \cdot V' \cdot N_A \cdot S_{a-Co(OH)_2} / S_{Si} = 1 \times 10^{-5} \text{ mol/L} \cdot 10 \times 10^{-6} \text{ L} \cdot$$

$$6.02 \times 10^{23} \text{ mol}^{-1} \cdot 4.8 \times 10^6 \text{ nm}^2 / (25 \times 10^6 \mu\text{m}^2) = 1.156 \times 10^7$$

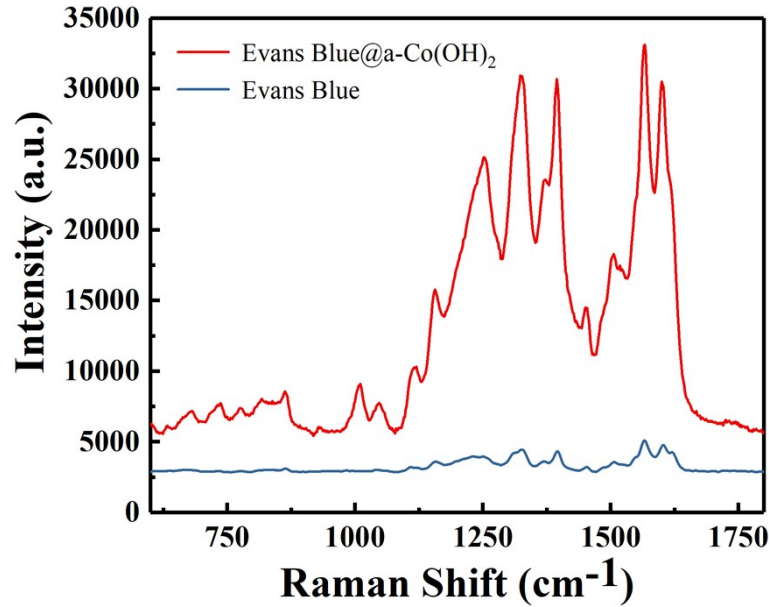


Figure S5. Raman spectrum of Evans Blue molecule at 0.1 M and SERS spectrum of Evans Blue molecule ($1 \times 10^{-5} \text{ M}$) adsorbed on a-Co(OH)₂ substrate.

I_{SERS} and I_{bulk} are based on the EB molecules vibration peak at 1565 cm^{-1} in SERS spectrum and normal Raman spectrum as shown in Figure S5, the intensity was obtained by making average 20 laser spots measurements, $I_{SERS} = 27731$ and $I_{bulk} = 2225$, also considering laser power for SERS and normal Raman. Substituting these

values of above variable into equation (1):

$$\begin{aligned} EF &= (I_{\text{SERS}}/I_{\text{bulk}}) \times (N_{\text{bulk}}/N_{\text{SERS}}) = (27731/2225) \times (1.445 \times 10^{11}/1.156 \times 10^7) \\ &= 1.56 \times 10^5 \end{aligned}$$

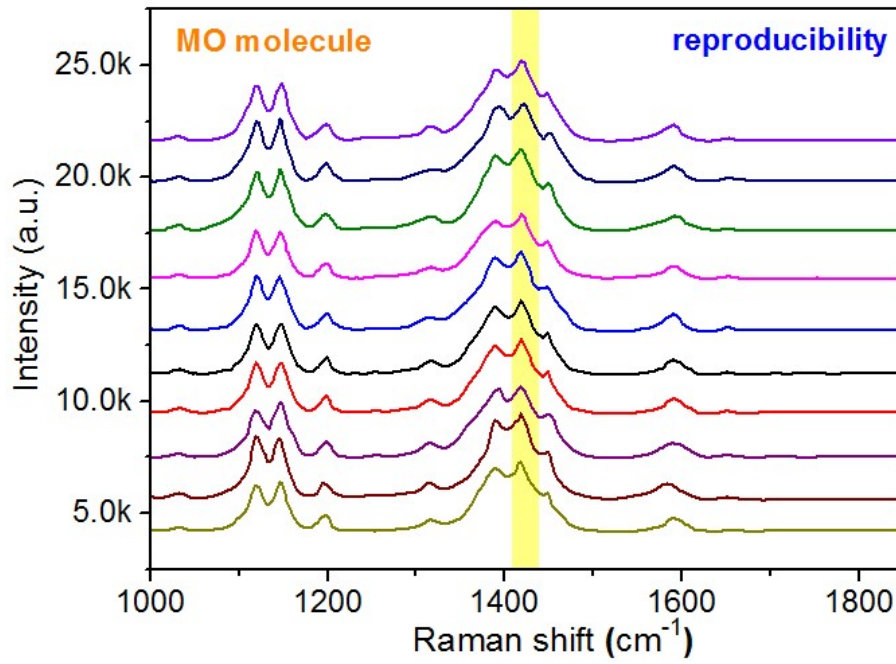


Figure S6. The SERS spectra of MO molecules acquired from ten different spots of a-Co(OH)₂ NCs substrate adsorbed by MO molecules (1×10^{-6} M).

We tested the SERS spectra of MO molecules at ten different positions of a-Co(OH)₂ NCs substrate adsorbed by Mo molecules. According to the formula:

$$c_v = \frac{\sigma}{\mu}$$

Where c_v is coefficient of variation; σ is standard deviation; μ is average value.

We can calculate the c_v of the intensity of the Raman characteristic peak of the MO

molecule at the position 1417 cm⁻¹. $c_v = \frac{\sigma}{\mu} = \frac{290.97}{3388.2} \approx 8.6\% < 10\%$, indicating that amorphous Co(OH)₂ nanocages exhibited excellent spectral reproducibility.

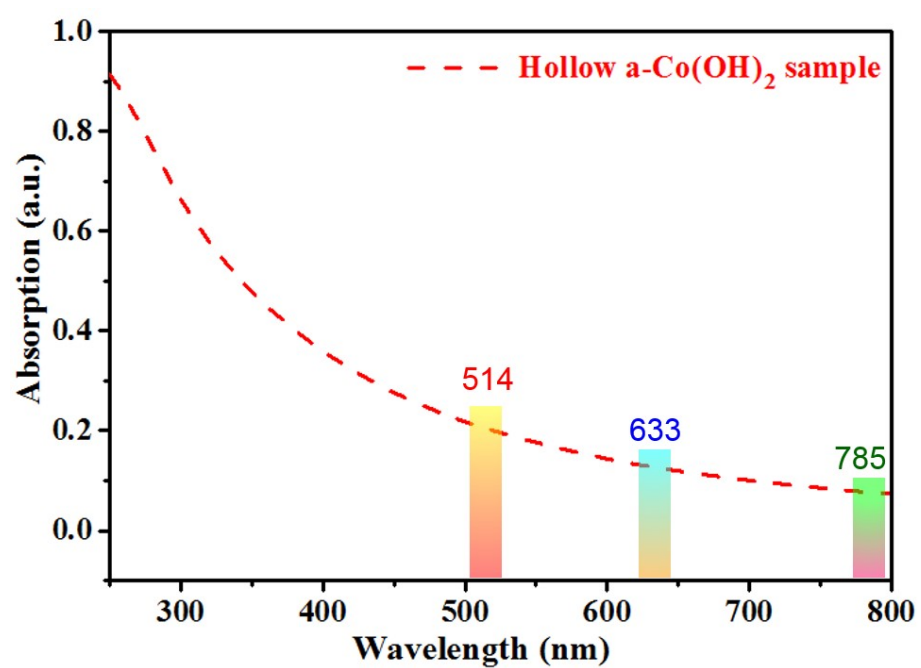


Figure S7. UV-Vis absorption spectrum of hollow a-Co(OH)₂ sample

First-principles density functional theory (DFT) simulation

The MO molecule structure was optimized by use of the B3LYP functional of the DFT methods that were implemented in the Gaussian 09 software package². The 6-311++G (d, p) basis set was used. The bandgap of MO molecules was taken as the different between its lowest unoccupied molecular orbital (LUMO) and the highest occupied molecular orbital (HOMO). The crystal structure of Co(OH)₂ was optimized using the Vienna ab initio simulation package (VASP)³⁻⁵. Projector augmented wave (PAW) potentials were used to treat ion-electron interactions, and the exchange-correlation contributions were treated by generalized gradient approximation (GGA), the Perdew-Burke-Ernzerhof (PBE) functional⁶. In the process of optimizing the lattice structure of Co(OH)₂ crystal, a conjugate gradient algorithm with a force tolerance of 0.01 eV/Å and a kinetic energy cutoff 500 eV was used to control the optimization convergence. The Gamma k-point sampling was set to be $5 \times 5 \times 5$.

The structure of amorphous Co(OH)₂ was obtained by AIMD simulations of VASP with Canonical ensemble (NVT) at 300K for 1000 fs for a $3 \times 3 \times 3$ supercell of Co(OH)₂. To further simulate adsorption of MO molecule and other molecular/racial intermediate products onto a-/c- Co(OH)₂, a 3×3 supercell was built by cutting the original cell along (100) facet, with a 25 Å additional vacuum layer added along the vertical direction. A six-layer slab was used to mimic Co(OH)₂ (100) surface, with the top three layers free to move, and bottom three layer fixed. For these supercell simulations, the plane wave cutoff energy set as 500 eV and the k-point mesh set as $1 \times 1 \times 1$. The bandgap of crystalline and amorphous structures of Co(OH)₂ was calculated as the difference between their conduction band minimum (CB) and valence band maximum (VB). For calculations of energy bands, the vacuum level was used as the benchmark. The DFT-D3 method with Becke-Jonson damping was adopted to include van der Waals interactions for surface/radical interactions. For the GGA+U correction⁷, the optimized U_{eff} ($U_{\text{eff}} = U - J$) for the Co atoms in was 3.3 eV. The charge transfers between MO and a-/c- Co(OH)₂ were analyzed by performing Bader charge analysis⁸ during electron self-consistent calculations.

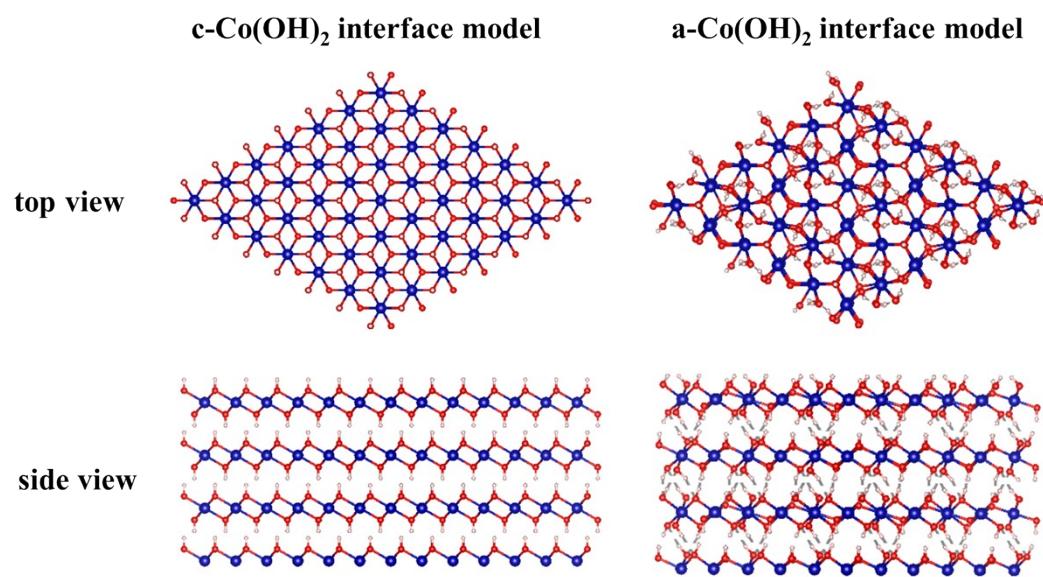


Figure S8. The top view and side view of a- and c-Co(OH)₂ interface models.

Table S1. Enhancement factor (EF) of various semiconductors in previous reports.

Material	Analyte	EF	Laser (nm)	Reference
a-Co(OH)₂ NCs	EB	1.56×10^5	514	this work
Amorphous Rh ₃ S ₆	R6G	1.02×10^5	647	Ref ⁹
few-layer MoS ₂	R6G	7.68×10^2	532	ref. ¹⁰
Ni(OH) ₂ microcages	MB	2.35×10^3	532	Ref ¹¹
Urchin-like W ₁₈ O ₄₉	R6G	3.4×10^5	522	Ref ¹²
TiO ₂ microarray	MB	2×10^4	532	Ref ¹³
H-Si/H-Ge	R6G/N719	8-28	532	Ref ¹⁴
Cu ₂ O nanosphere	4MBA	10^5	488	Ref ¹⁵
Li-MoS ₂	R6G	1.73×10^4	532	ref. ¹⁶
partially oxidized MoS ₂	R6G	1.4×10^5	532.8	Ref ¹⁷
WS ₂	R6G	2.5×10^4	532.8	Ref ¹⁷
ZnO Superstructures	4-MPy	10^5	532	Ref ¹⁸
MoO ₂	BPA	3.75×10^6	532.8	Ref ¹⁹
Mo-doped Ta ₂ O ₅	MV	2.2×10^7	532	Ref ²⁰

Table S2. O 1s peaks assignment for different bond species²¹.

Binding Energy	532.9 eV	532.0 eV	531.2 eV
Type of O species	O in H ₂ O	oxygen defect	O in Co-OH

Table S3. Brunauer-Emmett-Teller (BET) surface areas of the Cu₂O octahedrons, c-Co(OH)₂ and a-Co(OH)₂ NCs through N₂ adsorption-desorption test.

Sample	BET (m²/g)
Cu ₂ O octahedrons	5.0
c-Co(OH) ₂	18.3
a-Co(OH) ₂ NCs	20.0

References

1. D.-F. Zhang, H. Zhang, L. Guo, K. Zheng, X.-D. Han and Z. Zhang, *J. Mater. Chem.*, 2009, **19**, 5220-5225.
2. M. J. Frisch, G. Trucks, H. Schlegel, G. Scuseria, M. Robb, J. Cheeseman, G. Scalmani, V. Barone, B. Mennucci and G. Petersson, *Inc.: Wallingford, CT*, 2009.
3. G. Kresse and J. Hafner, *Phys. Rev. B*, 1994, **49**, 14251.
4. G. Kresse and J. Furthmüller, *Comp. Mater. Sci.*, 1996, **6**, 15-50.
5. G. Kresse and J. Furthmüller, *Phys. Rev. B*, 1996, **54**, 11169.
6. J. P. Perdew, K. Burke and M. Ernzerhof, *Phys. Rev. Lett.*, 1996, **77**, 3865.
7. L. Wang, T. Maxisch and G. Ceder, *Phys. Rev. B*, 2006, **73**, 195107.
8. W. Tang, E. Sanville and G. Henkelman, *J. Phys.-Condens. Mat.*, 2009, **21**, 084204.
9. A. Li, J. Lin, Z. Huang, X. Wang and L. Guo, *iScience*, 2018, **10**, 1-10.
10. B. P. Majee, S. Mishra, R. K. Pandey, R. Prakash and A. K. Mishra, *J. Phys. Chem. C*, 2019, **123**, 18071-18078.
11. M. Gao, P. Miao, X. Han, C. Sun, Y. Ma, Y. Gao and P. Xu, *Inorg. Chem. Front.*, 2019, **6**, 2318-2324.
12. S. Cong, Y. Yuan, Z. Chen, J. Hou, M. Yang, Y. Su, Y. Zhang, L. Li, Q. Li, F. Geng and Z. Zhao, *Nat. Commun.*, 2015, **6**, 7800.
13. D. Qi, L. Lu, L. Wang and J. Zhang, *J. Am. Chem. Soc.*, 2014, **136**, 9886-9889.
14. X. Wang, W. Shi, G. She and L. Mu, *J. Am. Chem. Soc.*, 2011, **133**, 16518-16523.
15. L. Jiang, T. You, P. Yin, Y. Shang, D. Zhang, L. Guo and S. Yang, *Nanoscale*, 2013, **5**, 2784-2789.
16. E. Er, H.-L. Hou, A. Criado, J. Langer, M. Möller, N. Erk, L. M. Liz-Marzán and M. Prato, *Chem. Mater.*, 2019, **31**, 5725-5734.
17. Z. Zheng, S. Cong, W. Gong, J. Xuan, G. Li, W. Lu, F. Geng and Z. Zhao, *Nat. Commun.*, 2017, **8**, 1993.
18. W. Ji, L. Li, W. Song, X. Wang, B. Zhao and Y. Ozaki, *Angew. Chem. Int. Ed.*, 2019, **58**, 14452-14456.
19. Q. Zhang, X. Li, Q. Ma, Q. Zhang, H. Bai, W. Yi, J. Liu, J. Han and G. Xi, *Nat. Commun.*, 2017, **8**, 14903.
20. L. Yang, Y. Peng, Y. Yang, J. Liu, H. Huang, B. Yu, J. Zhao, Y. Lu, Z. Huang, Z. Li and J. R. Lombardi, *Adv. Sci.*, 2019, **6**, 1900310.
21. J. Liu, J. Nai, T. You, P. An, J. Zhang, G. Ma, X. Niu, C. Liang, S. Yang and L. Guo, *Small*, 2018, **14**, 1703514.